AGU PUBLICATIONS

Geophysical Research Letters

RESEARCH LETTER
10.1002/2015GL067585

Key Points:
- Two-dimensional structures of daytime midlatitude sporadic *E* were imaged by InSAR and GPS-TEC
- Vortex structures were revealed, which were possibly generated by Kelvin-Helmholtz instability
- Small- and large-scale structures show similarity in their morphology

Correspondence to:
J. Maeda,
maeda@lib.hokudai.ac.jp

Citation:
Maeda, J., T. Suzuki, M. Furuya, and K. Heki (2016), Imaging the midlatitude sporadic *E* plasma patches with a coordinated observation of spaceborne InSAR and GPS total electron content, *Geophys. Res. Lett.*, *43*, 1419–1425, doi:10.1002/2015GL067585.

Received 28 DEC 2015
Accepted 2 FEB 2016
Accepted article online 5 FEB 2016
Published online 24 FEB 2016

Imaging the midlatitude sporadic *E* plasma patches with a coordinated observation of spaceborne InSAR and GPS total electron content

Jun Maeda[1], Takato Suzuki[2], Masato Furuya[2], and Kosuke Heki[2]

[1]Hokkaido University Library, Sapporo, Japan, [2]Department of Natural History Sciences, Hokkaido University, Sapporo, Japan

Abstract Kilometer-scale fine structures of midlatitude sporadic *E* (Es) plasma patches have been directly imaged for the first time by an interferogram derived from L band Advanced Land Observation Satellite/Phased Array-type L band Synthetic Aperture Radar data obtained over southwestern Japan. The synthetic aperture radar interferogram captured the eastern part of a large-scale frontal structure of daytime midlatitude E_s which spans over 250 km in the east-northeast to west-southwest direction. Fine structures are characterized by frontal and disc-shaped patches which are elongated in the same direction as the large-scale frontal structure. Length and width of the disc-shaped patches are 10–20 km and 5–10 km, respectively, and they are quasi-periodically located with a typical separation of 10–15 km. The Kelvin-Helmholtz instability with the vertical shear of zonal winds is considered to be the most likely candidate for the generation mechanism of the frontal patch and disc-shaped patches aligned in the zonal direction.

1. Introduction

Sporadic *E* (Es) is a thin densely ionized plasma patch, which often appears in the *E* region of the ionosphere most frequently during the local summer in midlatitude regions [*Whitehead*, 1989, and references therein]. Its unpredictable occurrence often degrades positioning accuracy of Global Navigation Satellite System (GNSS), such as Global Positioning System (GPS), by causing anomalous ionospheric delays of microwave signals. E_s also causes unusual long distance propagation of very high frequency waves.

Although the wind shear theory can well explain the formation of a thin layer by the vertical wind shears driven by zonal winds at midlatitudes [*Whitehead*, 1961], the formation mechanisms of E_s still remain elusive, because horizontal structures of E_s have long been unknown due to the lack of appropriate observation methods. *Miller and Smith* [1975, 1978] have inferred the horizontal structure of midlatitude E_s by using incoherent scatter radar. In recent years, two-dimensional (2-D) horizontal images of nighttime E_s have been revealed by ground-based radar observations using radio imaging technique [*Hysell et al.*, 2002, 2004; *Larsen et al.*, 2007]. *Hysell et al.* [2009] have used a coherent scatter radar at St. Croix, US Virgin Islands in the Caribbean Sea and shown patchy structures of nighttime E_s elongated in the east-west (E-W) and/or northwest-southeast (NW-SE) directions. The patches typically drifted perpendicularly to the elongation azimuth. *Saito et al.* [2006] have shown three-dimensional image of an E_s patch with an observation made by middle and upper atmosphere radar in Japan. *Kurihara et al.* [2010] have directly imaged the 2-D horizontal structure of an E_s patch by using the magnesium ion imager on board a rocket flying over southwestern Japan during the evening twilight. The patch had a horizontal dimension of 30 x 10 km elongated in the NW-SE direction. While majority of these observations are made during nighttime, *Maeda and Heki* [2014] have recently succeeded in the 2-D imaging of daytime midlatitude E_s with total electron content (TEC) observations using a dense network of GNSS receivers in Japan. They have shown several images of clear frontal structures extending in the E-W direction, spanning over 100 km.

While only a few observation reports of spatial structure of daytime E_s are available, there have been two major candidates to explain horizontal structuring of daytime E_s: atmospheric gravity waves [*Woodman et al.*, 1991; *Didebulidze and Lomidze*, 2010; *Chu et al.*, 2011] and the shear instability [*Larsen*, 2000; *Bernhardt*, 2002; *Larsen et al.*, 2007; *Hysell et al.*, 2009]. The atmospheric gravity waves are suggested to modulate E_s layer vertically, which would cause quasiperiodic (QP) radar echoes [*Yamamoto et al.*, 1991, 2005]. The shear instabilities in the neutral atmosphere such as the Kelvin-Helmholtz (KH) instability can also create a billow structure [*Bernhardt*, 2002], which has been imaged by *Larsen et al.* [2005] as a trimethyl aluminum trail. However,

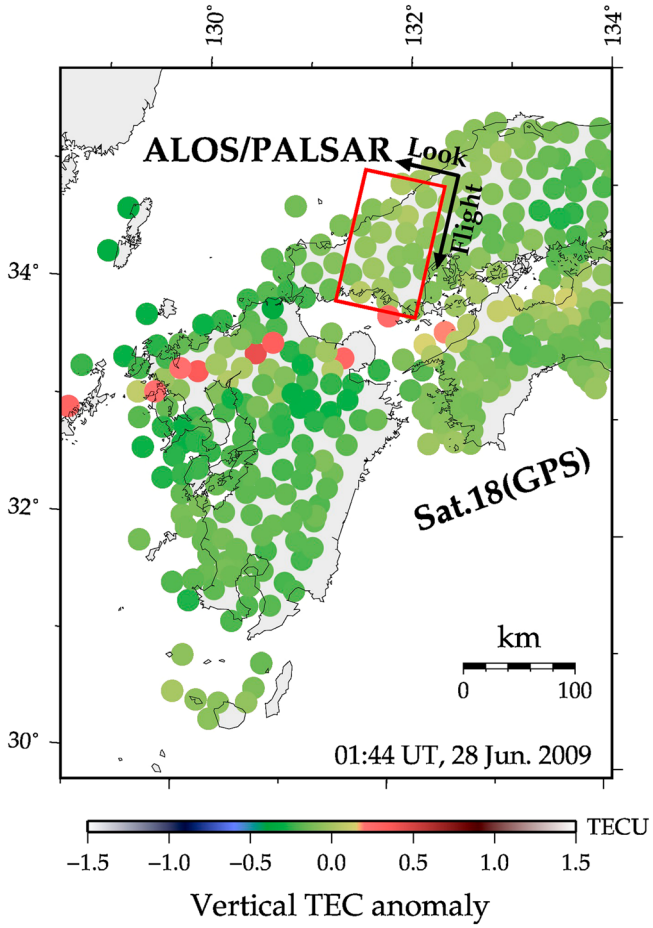

Figure 1. Vertical TEC anomaly map at 01:44 UT derived from GPS Satellite 18 when ALOS acquired the SAR image (red framed region). Vertical TEC anomaly map shows a large-scale frontal structure elongated over 250 km in the ENE-WSW direction. The SAR observation area corresponds to the eastern part of the frontal structure.

insufficient number of observations on horizontal structures, temporal evolution, and drifts of E_s has made it difficult to substantiate which mechanism is responsible for the formation of daytime E_s. In addition, coordinated observations on a horizontal structure of E_s by multiple techniques have been rarely performed despite the possible presence of E_s structures of multiple scales. Therefore, previous studies have been discussing only small- or large-scale structures depending on their observation techniques.

In the present study, we report the first result of direct imaging of both large- and small-scale plasma structures in daytime midlatitude E_s revealed by a coordinated observation through spaceborne interferometric synthetic aperture radar (InSAR) and GPS-TEC observation. Combination of InSAR and GPS-TEC allowed us for the first time to map the 2-D horizontal image of E_s in terms of both small- and large-scale structures. We will discuss possible instabilities operating in the E_s patches inferred from the horizontal structure.

2. Data and Analyses

2.1. InSAR Observation

We processed images acquired by Phased Array-type L band Synthetic Aperture Radar (PALSAR) of the Advanced Land Observation Satellite (ALOS) operated by Japan Aerospace Exploration Agency (JAXA). The operating frequency is 1270 MHz (wavelength of 23.6 cm). The recurrence interval of the ALOS was 46 days. The observation area is shown as a red rectangular region in Figure 1. From the two sets of ALOS/PALSAR level 1.0 raw data, acquired on 28 March 2009 (master image) and 28 June 2009 (slave image) both at 01:44 universal time (UT), we generated an interferogram whose spatial resolution is ~100 m.

Two major contributors to the interferometric phase difference are the effects of the spatial separation of the two orbits and the Earth's topography, which can be precisely corrected by the orbit data from JAXA and the 10 m digital elevation model by Geospatial Information Authority of Japan (GSI). InSAR images (interferograms) are primarily used to map crustal deformation due to, for example, earthquake [e.g., *Massonnet and Feigl*, 1998] and it is useful to detect dense water vapor blobs associated with heavy rainfalls as well [*Kinoshita et al.*, 2013]. Without these significant signals originated from crustal deformation and heavy rainfalls, InSAR can also image the differences of the TEC at the two epochs with unprecedented spatial resolution. In recent years, synthetic aperture radar (SAR) observations are used to observe *F* region ionospheric disturbances, e.g., medium-scale traveling ionospheric disturbances [*Pi et al.*, 2011]. In the present study, we try to map the 2-D image of E_s in the *E* region of the ionosphere. Before processing the SAR data, we confirmed that there were no earthquakes and heavy rain events in the observation area. We also confirmed that E_s is evident only on 28 June 2009 (slave image) and absent on 28 March 2009 (master image) by GPS-TEC observations. Thus, our results show the image of E_s occurred on 28 June 2009.

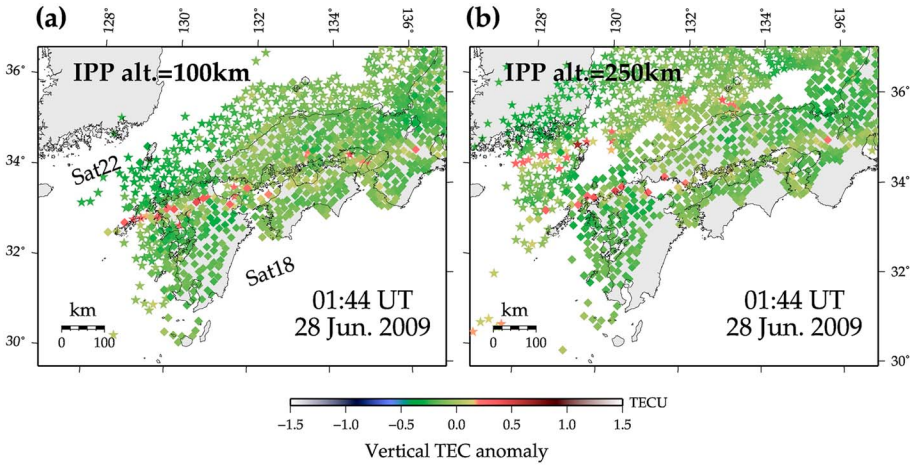

Figure 2. Altitude constraint by vertical TEC anomaly maps derived from two different satellites. Sub-ionospheric points (SIPs) of Satellite18 and Satellite 22 are represented by diamonds and stars, respectively. SIPs are projected by assuming the IPP altitude at (a) 100 km (*E* region height) and (b) 250 km (*F* region height). Looking at the ENE-WSW frontal structure, two images coincide in Figure 2a, while gaps emerge in Figure 2b. This ensures that the frontal structure exists at the altitude of *E* region of the ionosphere.

2.2. GPS-TEC Observation

The electron density in intensely ionized E_s patches, e.g., those with foEs more than 16 MHz, can exceed the peak density of the *F* region of the ionosphere. E_s patches cause extra ionospheric delays of microwaves and can be detected by TEC observations with dual frequency GNSS receivers [*Maeda and Heki*, 2014]. In this study, we analyzed GPS data from GNSS Earth Observation Network (GEONET), composed of ~1200 continuously operating receivers in Japan. GEONET is operated by GSI and the raw data are available online (www.terras.gsi.go.jp) upon request. Spatial resolution of a TEC map is ~15 km, reflecting typical horizontal separations of GNSS stations. The temporal resolution is 30 s.

One of the advantages of the GPS-TEC observation compared to InSAR is its larger spatial coverage and higher temporal resolution. GPS-TEC can observe the TEC above the ocean while InSAR cannot. Since GPS-TEC is based on one-way slanted line-of-sight signals between the satellite and the ground, it can observe

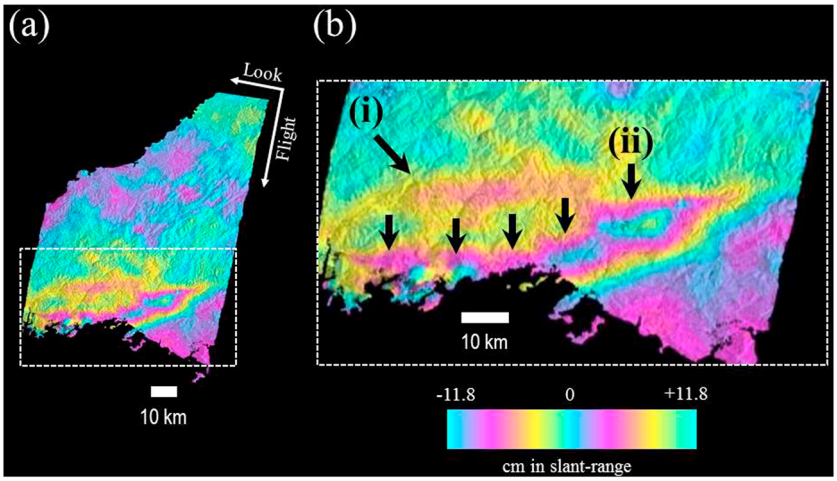

Figure 3. Interferogram derived from ALOS/PALSAR data (Path frame: 72–2920 ~ 2930). The phase changes are shown as slant range changes in centimeter. The cyclic color code is used to illustrate the spatial gradient of slant range changes. Beginning with pale blue, the color changes into purple and into yellow represent positive and negative slant range changes, respectively. (b) In an enlarged image, (i) a frontal patch (pointed by a slant arrow) and (ii) a chain of disc-shaped patches (pointed by short black arrows) are clearly seen.

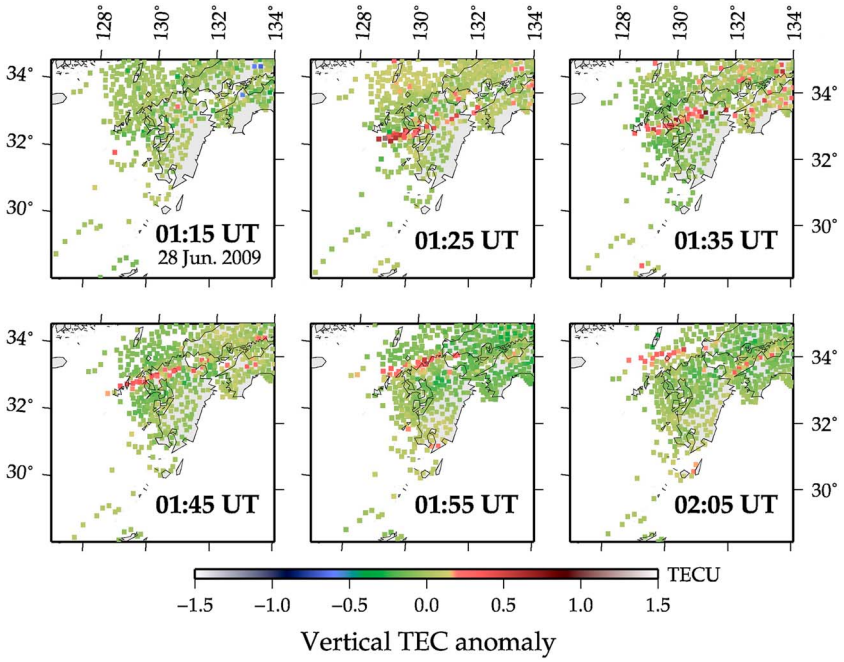

Figure 4. Snapshots of vertical TEC anomaly map derived from GPS Satellite 18 and 22 during 01:15 ~ 02:05 UT, including the observation time of SAR at 01:44 UT. The large-scale frontal structure migrated northward at the speed of 50–60 m/s.

TEC over the ocean. On the other hand, repeat-pass InSAR uses two-way propagation between the satellite and the ground to receive backscatter signals from the Earth's surface that must also be coherent at both master and slave acquisitions [*Hanssen*, 2001]. In contrast to those from the ground surface, backscatter signals from the sea surface are much weaker and incoherent between the two acquisition dates. Thus, we cannot observe TEC over the ocean by repeat-pass InSAR. In addition, the temporal resolution of GPS-TEC is much higher (e.g., 30 s for GEONET) than that of ALOS/PALSAR (its recurrence interval is 46 days). In the present study, we use both observation methods to achieve higher spatial and temporal resolution to reveal small-scale structure of E_s patches and their temporal evolution.

3. Results

3.1. Verification of Anomalous TEC and Phase Signals as Sporadic *E*

Figure 1 shows a snapshot of vertical TEC anomaly map at 01:44 UT on 28 June 2009, when the InSAR image (Figure 3) is acquired. The red rectangle represents the imaged area by ALOS/PALSAR which was on the descending (southward) orbit, looking (observing) the right side. In Figure 1, among the majority of green dots which show normal condition of the ionosphere, we can see some red dots indicating positive TEC anomalies. These electron density enhancements are confirmed to have occurred in the *E* region of the ionosphere by matching the vertical TEC anomaly maps derived from two different satellites (Figure 2) by the same procedure described in *Maeda and Heki* [2014]. In Figure 2, vertical TEC anomalies are projected by assuming the ionospheric penetration point (IPP) altitudes of 100 km (*E* region) and 250 km (*F* region). Looking at the frontal structure elongated in the ENE-WSW direction, the two images coincide when the IPP altitude is set to 100 km, while a large gap emerges with the IPP altitude of 250 km. Thus, the electron density enhancement is attributed to E_s.

Figure 3 shows the unwrapped InSAR image, where we can find several fringes, i.e., localized signal with large phase changes. The largest phase amplitude in the interferogram is approximately ~7 rad, which corresponds to ~0.5 total electron content (TEC) unit in L band [*Hanssen*, 2001]. This is almost consistent with the amplitude of vertical TEC anomalies, 0.5–1.0 TEC unit (Figure 1), observed by GPS-TEC.

3.2. Horizontal Structure

From the vertical TEC anomaly map (Figure 1), E_s patches imaged in the InSAR image correspond to the eastern part of a large-scale frontal structure. This frontal structure spans more than 250 km in the ENE-WSW direction

with the N-S width of ~20 km. It traveled northward at the speed of 50–60 m/s (Figure 4) when the SAR observation was made. Therefore, the northern (southern) edge of the frontal structure represents the leading (trailing) edge.

In Figure 3b, there are several small-scale patches. A belt-like frontal patch is evident in the north as indicated by a slant arrow labeled (i), followed by a few broken disc-shaped patches in the south (ii). Both frontal and disc-shaped patches are aligned/lined up in the ENE-WSW direction, which is the same azimuthal alignment as the large-scale frontal structure (Figure 1). The length and width of the frontal patch is ~25 km and ~5 km, respectively. As for disc-shaped patches, they are 10–20 km in E-W length and 5–10 km in N-S width and are horizontally separated by 10–15 km in the ENE-WSW direction. We call these patches quasiperiodic (QP) structures because of their quasiperiodic separation. The frontal patch and disc-shaped patches are separated by ~10 km in the N-S direction.

The phase changes of disc-shaped patches are much greater than that of the frontal patch. This indicates that the disc-shaped patches have larger electron density gradient than the frontal patch. It should also be noted that the leading (northern) edge of the disc-shaped patches are undulated in their borders, while the trailing (southern) edge looks smooth.

4. Discussion

Maeda and Heki [2015] have revealed that the E-W direction is the most commonly observed azimuthal alignment for large-scale frontal structures of daytime midlatitude E_s by GPS-TEC observations over Japan. As shown in Figure 3b, small-scale patches are elongated in the ENE-WSW direction, in the same azimuth as the large-scale frontal structure (Figure 1). This demonstrates a morphological similarity between the small- and large-scale structures. Why do the small-scale plasma patches and the large-scale frontal structure prefer to elongate in the E-W direction?

The wind shear theory is a widely accepted generation mechanism for the formation of E_s layer [*Whitehead*, 1960]. With inclined geomagnetic field lines at midlatitudes, the vertical shear of zonal winds drives upward and downward motion of metallic ions, at below and above an E_s layer, respectively [*Whitehead*, 1961, 1989]. For the generation mechanism of daytime E_s, there are two major candidates under the presence of such vertical wind shear: atmospheric gravity waves [*Woodman et al*., 1991; *Didebulidze and Lomidze*, 2010; *Chu et al*., 2011] and shear instability [*Larsen*, 2000; *Bernhardt*, 2002; *Larsen et al*., 2007; *Hysell et al*., 2009]. In Figure 3b, two E_s structures, i.e., frontal and disc-shaped patches, are separated only by ~10 km in the N-S direction. It indicates that atmospheric gravity waves are not likely to be the generation mechanisms of E_s patches shown here since atmospheric gravity waves have a horizontal wavelength of several tens of kilometers. Thus, we consider the possibility of shear instability as the formation mechanism of E_s observed in the present study.

In Figure 3b, both frontal patch and disc-shaped patches have the ENE-WSW alignment and almost the same scale size in the NNW-SSE direction. This indicates that the vertical shear of zonal winds is the primary driver for the formation of these E_s patches. Under the presence of vertical shear of zonal winds, frontal and disc-shaped patches are considered to be generated by shear instability. In fact, these two structures can be considered as vortexes or billows caused by shear instability because they have axes in the same direction, i.e., in ENE-WSW, with almost the same widths. *Larsen* [2000] has calculated wind shears based on direct measurements of wind speeds by rocket observations. It has been reported that the Richardson number can be lower than 0.25 between the zonal winds, which makes the neutral atmosphere susceptible enough to the KH instability [*Larsen*, 2000]. In the present case, two plasma structures, i.e., the frontal patch and disc-shaped patches, are considered to be generated at the two nodes of KH billows under the condition that the Richardson number is lower than 0.25, making the neutral atmosphere unstable to the KH instability. Since the axes of KH billows are perpendicular to the shear direction, two structures which are aligned in the ENE-WSW direction are suggested to be caused by a wind shear in the NNW-SSE direction. The ~10 km horizontal separation between the frontal patch and the disc-shaped patches is almost consistent with the KH wavelength of 8–10 km simulated by *Bernhardt* [2002]. Thus, it is suggested that the KH instability with the vertical shear of zonal winds causes ion perturbations in the neutral atmosphere, forming two KH billows aligned in the zonal direction.

In addition to the primary structuring of the two dominant structures, it is suggested that there could be a secondary instabilities operating in the southern disc-shaped patches. In Figure 3b, it is shown that disc-shaped

patches are more structured than the frontal patch in terms of the development of undulation in the northern leading edge and large electron density gradient. Although further justification is needed, there can be two major possibilities for the secondary development of the horizontal structure: the secondary turbulence in the neutral atmosphere [*Bernhardt*, 2002] and the plasma instabilities such as gradient-drift instability [*Kagan and Kelley*, 1998; *Kelley and Gelinas*, 2000]. Although we do not further discuss the secondary instability in this paper, more number of InSAR images on E_s and combined observations with in situ measurements on wind and electric field by such as rocket experiments will help to further determine these secondary instabilities possibly operating in the smaller-scale E_s patches.

Since the vertical wind shear is driven by $\mathbf{u} \times \mathbf{B}$ drift ($\mathbf{u}$ for the wind vector and $\mathbf{B}$ for the geomagnetic field), the plasma structure induced by the KH instability may have directional preference due to the direction of vertical wind shear and the direction of the geomagnetic field line. On the large-scale frontal structure, *Maeda and Heki* [2015] have shown that the E-W direction is the preferred alignment. Future work should be done to determine the directional preference of small-scale structures associated with daytime E_s.

5. Conclusions

In the present study, we have shown, for the first time, an InSAR image of plasma patches associated with daytime midlatitude E_s. This study can be concluded as follows:

1. The InSAR image revealed a detailed horizontal structure of E_s, i.e., a frontal patch and a series of disc-shaped patches embedded in the eastern part of a large-scale frontal structure.
2. Disc-shaped patches are quasi-periodically lined up in the ENE-WSW direction, which is the same elongation azimuth as the large-scale frontal structure. This suggests a morphological similarity between the small- and large-scale structures.
3. The KH instability with the vertical shear of zonal winds is the most likely candidate for the generation mechanism of the frontal patch and disc-shaped patches aligned in the ENE-WSW direction.
4. Disc-shaped patches form a quasiperiodic wavy structure, which have larger electron density gradient than the frontal patch. It is suggested that secondary instabilities may operate in the disc-shaped patches for the further small-scale structuring.

Acknowledgments
We thank Geospatial Information Authority of Japan for the GEONET data which are available online (www.terras.gsi.go.jp) upon request. The PALSAR level 1.0 data used in this study were provided by the PALSAR Interferometry Consortium to Study our Evolving Land surface (PIXEL) under cooperative research contracts between the Earthquake Research Institute at the University of Tokyo and JAXA. The PALSAR data belong to JAXA and the Ministry of Economy, Trade, and Industry. The authors would like to thank the two referees for their constructive reviews which have greatly improved the manuscript.

References

Bernhardt, P. A. (2002), The modulation of sporadic-*E* layers by Kelvin-Helmholtz billows in the neutral atmosphere, *J. Atmos. Sol. Terr. Phys.*, *64*, 1487–1504.

Chu, Y.-H., P. S. Brahmanandam, C.-Y. Wang, S. Ching-Lun, and R.-M. Kuong (2011), Coordinated sporadic *E* layer observations made with Chung-Li 30 MHz radar, ionosonde and FORMOSAT-3/COSMIC satellites, *J. Atmos. Sol. Terr. Phys.*, *73*, 883–894.

Didebulidze, G. G., and L. N. Lomidze (2010), Double atmospheric gravity wave frequency oscillations of sporadic E formed in a horizontal shear flow, *Phys. Lett. A*, *374*(7), 952–969.

Hanssen, R. F. (2001), *Radar Interferometry*, Kluwer Acad., Netherlands.

Hysell, D. L., M. Yamamoto, and S. Fukao (2002), Imaging radar observations and theory of type I and type II quasi-periodic echoes, *J. Geophys. Res.*, *107*(A11), 1360, doi:10.1029/2002JA009292.

Hysell, D. L., M. F. Larsen, and Q. H. Zhou (2004), Common volume coherent and incoherent scatter radar observations of mid-latitude sporadic E-layers and QP echoes, *Ann. Geophys.*, *22*, 3277–3290, doi:10.5194/angeo-22-3277-2004.

Hysell, D. L., E. Nossa, M. F. Larsen, J. Munro, M. P. Sulzer, and S. A. González (2009), Sporadic *E* layer observations over Arecibo using coherent and incoherent scatter radar: Assessing dynamic stability in the lower thermosphere, *J. Geophys. Res.*, *114*, A12303, doi:10.1029/2009JA014403.

Kagan, L. M., and M. C. Kelley (1998), A wind-driven gradient drift mechanism for midlatitude E region ionospheric irregularities, *Geophys. Res. Lett.*, *25*, 4141–4144, doi:10.1029/1998GL900123.

Kelley, M. C., and L. J. Gelinas (2000), Gradient drift instability in midlatitude sporadic E layers: Localization of physical and wavenumber space, *Geophys. Res. Lett.*, *27*, 457–460, doi:10.1029/1999GL900604.

Kinoshita, Y., M. Shimada, and M. Furuya (2013), InSAR observation and numerical modeling of the water vapor signal during a heavy rain: A case study of the 2008 Seino event, central Japan, *Geophys. Res. Lett.*, *40*, 4740–4744, doi:10.1002/grl.50891.

Kurihara, J., et al. (2010), Horizontal structure of sporadic *E* layer observed with a rocket-borne magnesium ion imager, *J. Geophys. Res.*, *115*, A12318, doi:10.1029/2009JA014926.

Larsen, M. F. (2000), A shear instability seeding mechanism for quasiperiodic radar echoes, *J. Geophys. Res.*, *105*, 24,931–24,940, doi:10.1029/1999JA000290.

Larsen, M. F., M. Yamamoto, S. Fukao, and R. T. Tsunoda (2005), SEEK 2: Observations of neutral winds, wind shears, and wave structure during a sporadic E/QP event, *Ann. Geophys.*, *23*, 2369–2375.

Larsen, M. F., D. L. Hysell, Q. H. Zhou, S. M. Smith, J. Friedman, and R. L. Bishop (2007), Imaging coherent scatter radar, incoherent scatter radar, and optical observations of quasiperiodic structures associated with sporadic *E* layers, *J. Geophys. Res.*, *112*, A06321, doi:10.1029/2006JA012051.

Maeda, J., and K. Heki (2014), Two-dimensional observations of midlatitude sporadic *E* irregularities with a dense GPS array in Japan, *Radio Sci.*, *49*, 28–35, doi:10.1002/2013RS005295.

Maeda, J., and K. Heki (2015), Morphology and dynamics of daytime mid-latitude sporadic-E patches revealed by GPS total electron content observations, *Earth Planets Space*, *67*, 89, doi:10.1186/s40623-015-0257-4.

Massonnet, D., and K. L. Feigl (1998), Radar interferometry and its application to changes in the Earth's surface, *Rev. Geophys.*, *36*(4), 441–500, doi:10.1029/97RG03139.

Miller, K. L., and L. G. Smith (1975), Horizontal structure of mid-latitude sporadic *E* layers observed by incoherent scatter radar, *Radio Sci.*, *10*, 271–276, doi:10.1029/RS010i003p00271.

Miller, K. L., and L. G. Smith (1978), Incoherent scatter radar observations of irregular structure in mid-latitude sporadic *E* layers, *J. Geophys. Res.*, *33*, 3761–3775, doi:10.1029/JA083iA08p03761.

Pi, X., A. Freeman, B. Chapman, P. Rosen, and Z. Li (2011), Imaging ionospheric inhomogeneities using spaceborne synthetic aperture radar, *J. Geophys. Res.*, *116*, A04303, doi:10.1029/2010JA016267.

Saito, S., M. Yamamoto, H. Hashiguchi, and A. Maegawa (2006), Observation of three-dimensional structures of quasi-periodic echoes associated with mid-latitude sporadic-*E* layers by MU radar ultra-multi-channel system, *Geophys. Res. Lett.*, *33*, L14109, doi:10.1029/2005GL025526.

Whitehead, J. D. (1960), Formation of the sporadic *E* layer in the temperate zones, *Nature*, *188*, 567.

Whitehead, J. D. (1961), The formation of the sporadic *E* layer in the temperate zone, *J. Atmos. Terr. Phys.*, *20*, 49–58.

Whitehead, J. D. (1989), Recent work on mid-latitude and equatorial sporadic *E*, *J. Atmos. Terr. Phys.*, *51*, 401–424.

Woodman, R. F., M. Yamamoto, and S. Fukao (1991), Gravity wave modulation of gradient drift instabilities in mid-latitude sporadic *E* irregularities, *Geophys. Res. Lett.*, *18*, 1197–1200, doi:10.1029/91GL01159.

Yamamoto, M., S. Fukao, R. F. Woodman, T. Ogawa, T. Tsuda, and K. Kato (1991), Mid-latitude *E*-region field aligned irregularities observed with the MU radar, *J. Geophys. Res.*, *96*, 15,943–15,949, doi:10.1029/91JA01321.

Yamamoto, M., S. Fukao, R. T. Tsunoda, R. Pfaff, and H. Hayakawa (2005), SEEK-2 (Sporadic-*E* Experiment over Kyushu 2)—Project outline, and significance, *Ann. Geophys.*, *23*, 2295–2305, doi:10.5194/angeo-23-2295-2005.